

Short-time SSVEP data extension by a novel generative adversarial networks based framework

Yudong Pan¹, Student Member, IEEE, Ning Li¹, Yangsong Zhang¹

Abstract—Objective: Steady-state visual evoked potentials (SSVEPs) based brain-computer interface (BCI) has received considerable attention due to its high transfer rate and available quantity of targets. However, the performance of frequency identification methods heavily hinges on the amount of user calibration data and signal data length, which hinders the deployment in real-world applications. Recently, generative adversarial networks (GANs)-based data generation methods have been widely adopted to create supplementary synthetic electroencephalography (EEG) data, holds promise to address these issues. **Methods:** In this paper, we proposed a GAN-based end-to-end signal transformation network for data length window extension, termed as TEGAN. TEGAN transforms short-time SSVEP signals into long-time artificial SSVEP signals. By incorporating a novel U-Net generator architecture and auxiliary classifier into the network design, the TEGAN could produce conditioned features in the synthetic data. Additionally, to regularize the training process of GAN, we introduced a two-stage training strategy and the LeCam-divergence regularization term during the network implementation. **Results:** The proposed framework was evaluated on two public SSVEP datasets. With the assistance of TEGAN, the performance of traditional frequency recognition methods and deep learning-based methods have been significantly improved under limited calibration data. **Conclusion:** This study substantiates the feasibility of the proposed method to extend the data length for short-time SSVEP signals to develop a high-performance BCI system. **Significance:** The proposed GAN-based methods have the great potential of shortening the calibration time for various real-world BCI-based applications, while the novelty of our augmentation strategies shed some value light on understanding the subject-invariant properties of SSVEPs.

Index Terms—brain-computer interface (BCI), steady-state visual evoked potential (SSVEP), electroencephalography (EEG), generative adversarial network (GAN)

I. INTRODUCTION

RAIN-COMPUTER interface (BCI) has shown to become a promising technology that can provide its users with communication channels that do not depend on conventional output channels of peripheral nerves and muscles by decoding their neural activities into specific control commands [1]. Among various neuroimaging modalities to implement a BCI system, electroencephalography (EEG) has been the most prominent signal accounting for such the advantages as non-invasiveness, high temporal resolution, affordability, ease of implementation, portability, and convenience of use [2], [3].

Several most popular paradigms can be employed to build EEG-based BCI systems, such as motor imaginary (MI) [4], P300 event

This work was supported in part by the National Natural Science Foundation of China under Grant No.62076209.

Y. Pan is with the School of Computer Science and Technology, Southwest University of Science and Technology, Mianyang 621010, China (e-mail: panydacademy@163.com).

N. Li is with the School of Computer Science and Technology, Southwest University of Science and Technology, Mianyang 621010, China (e-mail: liningacademy@163.com).

Y. Zhang is with the School of Computer Science and Technology, Southwest University of Science and Technology, Mianyang 621010, China, and also with MOE Key Laboratory for Neuroinformation, Clinical Hospital of Chengdu Brain Science Institute, University of Electronic Science and Technology of China, Chengdu 610054, China (e-mail:zhangysacademy@gmail.com).

related potentials (P300) [5], auditory steady-state response (ASSR) [6], and steady-state visual evoked potential (SSVEP) [7]. Among them, SSVEP-based BCI systems have received considerable attention due to its high transfer rate (ITR) and available quantity of targets. SSVEPs refer to periodic evoked potentials over occipital scalp areas, in response to rapidly repetitive visual stimulation flicking or reversing at a specific frequency [8]. The SSVEP signal consists of a number of discrete frequency components, normally including the fundamental frequency of the visual stimulus and its harmonics. On the strengths and characteristics of SSVEP, numerous SSVEP-based BCI applications have been developed, such as bionic mechanical leg [9], unmanned aerial vehicle [10], dial interface [11], high-speed mental speller [12], smart homes [13], and games [14]. To design a high-performance BCI system based on SSVEP signal, the most crucial aspect is to develop a fast and accurate frequency recognition method that can distinguish the stimulus frequency of the target gazed by the users through analyzing the EEG signal in the shortest possible time. Thus, various cutting-edge algorithms have been proposed based on different perspectives.

Generally, the frequency identification algorithms can be divided into three categories: training-free methods, user-dependent (UD) training methods and user-independent (UI) training methods [15]. Training-free identification methods do not require any training data from the user of the BCI, from which the user can interact directly with the system. The representative training-free methods are canonical correlation analysis (CCA) [7] and multivariate synchronization index (MSI) [16]. CCA seeks to capture the underlying correlation between EEG data and a series of sinusoidal reference templates corresponding to the stimuli frequencies, while MSI adopts the S-estimator to estimate the synchronization index. CCA and MSI are able to achieve comparable performance when only a few stimulus targets are available and the EEG signals are sufficiently long, but their performance drops dramatically when encountering a large number of targets and short-time signals [17]. By incorporating the user-specific training data into the algorithm design, the UD methods could derive better performance than training-free methods under these harsh conditions. The UD approaches take the discrimination of recorded signals from different subjects into account, namely subject-variant features, such as magnitude, phase, and visual latency. Draw support from individual training data to learn these properties, the performance of recognition algorithm would be greatly improved. The typical UD algorithms mainly comprise individual template CCA (ITCCA) [18], multiway CCA (MCCA) [19], task-related component analysis (TRCA) [20], and correlated component analysis (CORCA) [21], etc. In contrast to the UD methods, UI methods are envisaged to build a generalized model for detection of unseen subjects via studying the subject-invariant features that learning from the existing subject datasets or human prior knowledge. For UI algorithms, subject-specific training data is not required. However, their performance usually is worse than UD algorithms. Theoretically, training-free algorithms are all belong to UI methods for their user-independent properties. The prevalent UI approaches include filter bank canonical correlation analysis (FBCCA) [22], transfer template-based canonical correlation analysis (ttCCA) [23]

and adaptive combined CCA (A3C) [24], etc.

Although UD approaches commonly exhibit better performance than UI algorithms, they are heavily dependent on the amount of collected user-specific calibration data. Actually, collecting user calibration data is a time-consuming and laborious process, and prolonged experiments would cause user's fatigue, leading to the decreased quality of induced SSVEP signals. Hence, how to develop a high-performance frequency recognition algorithm that needs only a little calibration data or calibration-free has become a hot research topic in recent years [23], [25]–[28]. Benefit from the rapid development of deep learning (DL) in the past decade, there has been an increased interest in applying DL algorithms to detect SSVEPs for BCI researchers. In view of powerful feature representation capacity and flexibility, the DL-based methods hold promise for reducing the gap between UD approaches and UI approaches. For instance, Waytowich et al. employed a compact convolutional neural network (Compact-CNN) entitled EEGNet to conduct inter-subject classification, which yielded about 80% accuracy in a 12-class SSVEP dataset without any user calibration data [29]. Ravi et al. utilized fast Fourier transform (FFT) to design a complex spectrum CNN (C-CNN) which could be trained on both UD and UI schemes, achieving about 92.5% (UD), 81.6% (UI) and 92.3% (UD), 81.6% (UI) accuracy on a 12-class and a 7-class SSVEP dataset, respectively [30]. Guney et al. proposed a two-stage training strategy and a deep neural network (DNN) to improve performance of intra-subject classification [31]. The proposed framework was evaluated on Benchmark SSVEP dataset that contains 40 stimulus targets, and has obtained approximately 95% recognition accuracy. Pan et al. developed an efficient CNN-LSTM (Long short-term memory) network with spectral normalization and label smoothing technologies, termed as SSVEPNet, for SSVEP classification under the small sample size and short-time window scenarios [32]. SSVEPNet was verified on a 4-class and a 12-class SSVEP dataset, yielding about 88.5% identification accuracy when a few trials of each stimulus are available. Chen et al. introduced a Transformer-based deep neural network model named SSVEPformer for enhancing the performance of zero-calibration SSVEP-BCI [33]. The experimental results have shown that SSVEPformer could achieve high accuracy of about 84% and 80% on a 12-class and Benchmark SSVEP dataset.

On the other hand, in addition to explicitly modelling an efficient frequency recognition method that requires less calibration data, recent studies have substantiated the potential of using the generative models to address the issues of data shortage in the SSVEP classification tasks [34]. Generative models aim to learn the distribution of real data by constructing a probabilistic statistical model given real data and using it to generate synthetic data that approximate the distribution of real data [35]. Autoregressive models [36], variational auto-encoder (VAE) [37], generative adversarial network (GAN) [38], and denoising diffusion probabilistic model (DDPM) [39] are the most commonly generative models. Among them, GAN has been the most widely applied technique to synthesize fake data and overcome the problem of limited data. Since EEG-GAN [40], the first GAN-based generative model of EEG signal, was proposed in 2018, BCI researchers have successively developed several GAN-based SSVEP generation models. In 2019, Aznan et al. firstly exploited the GAN-based generative model in circumventing the limited calibration data via generating supplementary synthetic data to enlarge the size of training data [41]. Only one year later, they also proposed a subject-invariant SSVEP GAN (SIS-GAN) to generate artificial EEG data that learns the subject-invariant features from the multiple SSVEP categories [42]. After two years, inspired by StarGAN v2, which has been used to solve multidomain image-to-image conversion, Kwon et al. proposed a novel multidomain signal-to-signal transformation

method which is capable of generating artificial SSVEP signals from resting EEG [43].

Although these GANs based on SSVEP signals have made noticeable progress, these studies only focus on generating simulated data to enlarge the amount of the training dataset, without considering the extension of signal length. However, longer SSVEP signal length would often achieve more accurate recognition results under the same conditions [30]–[33]. Hence, in this study, we proposed a GAN-based end-to-end signal transformation network for data length window extension, termed as TEGAN. TEGAN transforms short-time SSVEP signals into long-time artificial SSVEP signals. By incorporating a novel U-Net generator architecture and auxiliary classifier into the network design, the TEGAN could produce conditioned features in the synthetic data. Additionally, to regularize the training process of GAN, we introduced a two-stage training strategy and the LeCam-divergence regularization term during the network implementation. The proposed methods were evaluated on two public SSVEP datasets. With the assistance of TEGAN, the performance of traditional frequency recognition methods and DL-based methods have been significantly improved under limited calibration data. The extensive experimental analysis demonstrates the effectiveness of the proposed methods, while the novelty of our augmentation strategies shed some value light on understanding the subject-invariant properties of SSVEPs.

II. METHODOLOGY

A. Dataset

In this study, two public SSVEP datasets were employed to evaluate the proposed augmentation methods. According to the design purpose of these two datasets, we hereinafter termed them as Direction SSVEP dataset and Dial SSVEP dataset, respectively. The specific details of each dataset are described as follows:

1) Direction SSVEP dataset: This dataset was published by Lee et al. in 2019 [44]. Fifty-four healthy subjects (25 females, aged 24–35 years) participated in the experiment. The experiment collected EEG data of subjects in two different periods (Session1 and Session2), and the data in each period was divided into offline analysis stage and online testing stage. For the sake of simplicity, the offline data from Session1 was chosen for experimental evaluation in this study.

In the process of data acquisition, the four target stimuli were coded by 5.45 Hz, 6.67 Hz, 8.57 Hz and 12 Hz, and played in the lower, right, left and upper directions of the personal computer (PC) display, respectively. Participants were asked to focus on the center of the black screen, and then on the direction of the target stimulus highlighted in different colors. Each SSVEP stimulus was presented for 4 s, and the interval between two stimuli was 6 s. Each target frequency was presented 25 times, leading to a total of 100 trials (4 classes \times 25 trial). EEG data of 62 Ag/AgCl electrodes collected at a sampling rate of 1000 Hz were recorded in the experiment. Ten electrodes (P7, P3, Pz, P4, P8, PO9, PO10, O1, Oz and O2) covering the occipital lobe area were selected for our research. All data was down sampled to 100 Hz and band-pass filtered between 4 and 40 Hz through a fourth-order Butterworth band-pass filter.

2) Dial SSVEP dataset: This open access dataset was provided by Nakanishi et al. in 2015 [11]. In this dataset, ten healthy subjects (1 female, mean age: 28 years) participated in the experiment. The subjects were instructed to sit in a comfortable chair 60 cm in front of a liquid crystal display (LCD) monitor in a dim room. The stimuli were arranged in a 4×3 grid space as simulation a dial interface. Twelve flickering stimuli ($f_0 = 9.25\text{Hz}$, $\Delta f = 0.5\text{Hz}$) were presented on the monitor. The EEG data of eight Ag/AgCl electrodes (PO7, PO3, POZ, PO4, PO8, O1, Oz and O2) covering the occipital were acquired using

the BioSemi ActiveTwo EEG system with a sampling rate of 2048 Hz. For each subject, there were 15-run experiments. In each run, 12 trials corresponding to all 12 stimuli were generated in a random order. Thus, a total of 180 trials were collected in the experiment. Each trial was composed of 1 s cuing period and 4 s targeted flickering period.

All data was down sampled to 256 Hz and band-pass filtered between 6 and 80 Hz through a fourth-order Butterworth band-pass filter. To suppress the adverse effect of visual latency, the data was extracted from the 135 ms after the stimulus onset.

B. Frequency recognition methods

In this subsection, we briefly introduce two traditional frequency recognition methods and two DL-based methods. All of these state-of-the-art methods were adopted as baselines to verify the effectiveness of the proposed methods.

1) Traditional Methods:

- **IT-CCA:** CCA is a multivariate statistical technique to search the underlying correlation between two multidimensional variables, by calculating a pair of weight vectors to maximize the Pearson's correlation coefficients between their linear combinations. For CCA-based SSVEP recognition methods, the coefficient is calculated between the multi-channel EEG data and the artificial reference signal [7]. However, the artificial reference signals lack the specific characteristics of subjects. Then, IT-CCA was proposed to substitute the artificial reference signal for individual template reference signal obtained by averaging multiple training trials of specific subject [18]. This strategy has been proved to be able to suppress spontaneous EEG interference and achieve better classification performance than CCA algorithm.
- **TRCA:** TRCA is a method which learns the spatial filters to extract task related components by maximizing the reproducibility of neuroimaging data during the task period [45]. For SSVEP data, TRCA seeks to find a linear weight vector to maximize the inter-trial correlation of its linear combinations, referring as task-related components. In 2018, Nakanish *et al.* first applied TRCA algorithm to build a high-speed SSVEP-based BCI system [20]. In the literature, TRCA is extended with the filter bank technique, and the selection of filter banks follows the principle proposed by Chen *et al.* [22]. For better comparison with other methods, the original TRCA algorithm without filter bank technology was adopted in the current study.

2) DL-based methods:

- **EEGNet:** EEGNet is a robust DL model which could yield comparable performance across multiple EEG tasks and datasets [46]. It is mainly comprised of a temporal filtering layer, a depthwise convolution layer, a separable convolution layer, and a fully connected layer. Among these network components, depthwise and separable convolution make the model become compact and efficient. Due to its effectiveness, Waytowich *et al.* used EEGNet to decode SSVEP signals for inter-subject classification on Dial SSVEP dataset, and has achieved about 80% accuracy [29].
- **C-CNN:** The frequency domain of SSVEP data contains abundant frequency and phase information relevant to the recognition task. If this information could be adequately exploited, the classification performance could be further improved. Therefore, Ravi *et al.* utilized FFT to transform SSVEP signals from the time domain to the frequency domain and designed a shallow CNN consisting of a spatial filter layer, a convolutional layer, and a fully connected layer to handle complex spectral data [30].

C-CNN was evaluated on a 7-class and Dial SSVEP dataset, yielding satisfactory results for both intra- and inter-subject classification.

C. The proposed augmentation methods

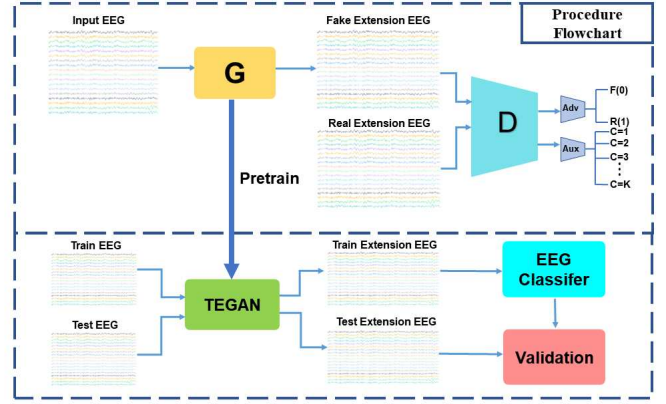


Fig. 1: The procedure flowchart of the proposed augmentation method. The whole process is divided into two steps. In the first step, real short EEG and real long EEG of training dataset are used to train the GAN model. In the second step, the pretrained generator is employed to transform all input short EEG into synthetic long EEG. Then the synthetic long EEG are used to train the EEG classifier and conduct classification.

1) Overall framework: The procedure flowchart of the proposed augmentation method is illustrated in Fig. 1. The whole process is divided into two steps. In the first step, we train the TEGAN, which could transform short time-window natural EEG into long time-window artificial EEG. Concretely, followed by the auxiliary classifier GAN (ACGAN) paradigm [47], TEGAN mainly includes two components, i.e., a generator and a discriminator, competing in a zero-sum game. The generator receives the real short EEG as network input, then output the extended EEG data, namely long artificial EEG data. The discriminator is responsible for distinguishing between long real EEG data and long fake EEG data and simultaneously identifying their respective classes. Let V_G and V_D denote the training objectives of the generator G and discriminator D , respectively. Then the training of the proposed GAN frameworks can be generally expressed as:

$$\min_G V_G = \mathbb{E}_{x \sim p_{x_s}} [-D(G(x))] - \mathbb{E}_{x \sim p_{x_s}} [\log(D(G(x) \in C))] \quad (1)$$

$$\begin{aligned} \max_D V_D = & \mathbb{E}_{x \sim p_{x_l}} [1 - D(x)] + \mathbb{E}_{x \sim p_{x_s}} [1 + D(G(x))] \\ & + \mathbb{E}_{x \sim p_{x_l}} [\log(D(x) \in C)] + \mathbb{E}_{x \sim p_{x_s}} [\log(D(G(x) \in C))] \end{aligned} \quad (2)$$

where p_{x_s} and p_{x_l} is the data distribution of short EEG data and long EEG data from the training dataset, respectively. The notation $D(x \in C)$ represents the probability of the class label being correctly identified.

To optimize these two objective functions, we use gradient descent algorithm to train discriminator and generator alternately, and obtain the optimal parameters of generator θ_G^* . Hence, a short-to-long signal converter $\zeta(\cdot)$ could be constructed using θ_G^* as follows:

$$\zeta(x_s) = G(x_s | \theta = \theta_G^*) = x_l \quad (3)$$

In the second step, the converter $\zeta(\cdot)$ is employed to transform all short EEG into synthetic long EEG. Finally, the synthetic long EEG are used to train the EEG classifier and conduct classification. It is worth noting that since the converter is trained using only the training dataset and does not require label information as input, there is no data leakage problem during the entire operation. The implementation code of TEGAN would be available in Github platform.

2) The architecture of generator: The detailed architecture of generator is presented in Fig. 2. The whole architecture of the generator follows the U-Net architecture proposed by Ronneberger et al. [51], which is divided into down sampling stages and up sampling stages. Moreover, considering the dependency between spatial-temporal features of EEG data, we utilize a bidirectional long short-term memory (Bi-LSTM) network to encode the features derived by the last down-sampling module, thus connecting the down sampling stages and up sampling stages. Furthermore, we added a conditional batch normalization (cBN) layer in each up-sampling module to mitigate the adverse effects of homogenization between different synthetic samples [50]. However, due to the inaccessibility of label information in the input end of generator, we adopted a fully connected layer to create high-confidence pseudo label, which can be improved via minimizing the following objective function L_G :

$$\min_G L_G = V_G - \sum_{c=1}^K y_c \log p_c \quad (4)$$

where y_c is realistic label with one-hot encoding, p_c is the predicted probability of class c , and K is number of classes.

The network parameters of generator are exhibited in Table I. Among the parameters, the kernel size DK for down-sampling module could be determined through the following formula:

$$DK_i = \lceil D_i * ws \rceil, i = 1, 2, 3 \quad (5)$$

where $D = \{20, 12, 8\}$, and ws represents the window size of input short EEG signal. Then the kernel size UK for up-sampling module could be calculated as:

$$UK_{i+1} = DT_{2-i} - (DT_{3-i}) * S_i, i = 0, 1, 2 \quad (6)$$

Here, $S = \{1, 2, 2\}$, and DT represents the number of time steps for down sampling module, which is presented in Table I.

3) The architecture of discriminator: The minute architecture of discriminator is shown in Fig. 3. Overall, the discriminator follows the design of our previously proposed SSVEPNet model [32]. It is mainly comprised of three modules, namely spatial filtering module, temporal filtering module, and decision module. In the spatial filtering module, a one-dimensional convolution (1D Conv) layer is used to fuse different channel information of EEG. In the temporal filtering layer, 1D Conv layer is employed to extract temporal features of EEG. In the decision module, a Bi-LSTM layer is leveraged to learn the dependence between spatial-temporal features, while fully connected layers are employed for classification and authentication. The distinction between SSVEPNet and proposed discriminator only lies in two points. One is that a max pooling layer with a kernel size of 2 has been added to the temporal filtering module. Another is that the fully connection layer in the decision module has changed from three layers to two layers, and the neurons in the first layer is equal to twentieth of encoded spatial-temporal features outputted by BiLSTM layer. The remaining network parameters of the discriminator are identical with SSVEPNet.

4) Regularizing TEGAN on limited data: GAN is notoriously difficult to train, it is highly susceptible to encounter with mode collapse phenomenon - particularly from datasets with high variability. Furthermore, this problem may deteriorate with a limited training data. Generators are inclined to merely memorize limited training samples, rather than learning the sophisticated data distribution of training dataset [47]. To moderate this issue, we introduce a two-stage training strategy and LeCam divergence regularization term to regularize the training process of TEGAN.

Firstly, inspired by the previous study [31], we utilized transfer learning technique to design a two-stage training strategy for the proposed GAN framework. In the first stage, we train two global models D_s and G_s using the cross-subject data. In the second stage, the network parameters of D_s and G_s are directly duplicated to two target models, D_t and G_t . Then we freeze the parameters in D_t in addition to the fully connection layers, and fine-tune D_t and G_t using a limited amount of training data of target subjects.

Secondly, we supplemented a LeCam regularization term in the training objective of discriminator, which has been substantiated that could offer meaningful constraints under limited training data [52]:

$$\min_D L_D = V_D + \lambda R_{LC}(D) \quad (7)$$

where λ represents regularization term, and LeCam regularization term $R_{LC}(D)$ is expressed as:

$$R_{LC}(D) = \mathbb{E}_{x \sim p_{x_l}} [\|D(x) - \alpha_F\|^2] - \mathbb{E}_{x \sim p_{x_s}} [\|D(G(x)) - \alpha_R\|^2] \quad (8)$$

where α_F and α_R are anchors obtained by the exponential moving average variables, which is aiming at tracking the discriminator predictions. Assuming that there are TE training epochs in total, then α_F and α_R could be calculated using the following equations:

$$\begin{cases} \alpha_F(i+1) = \gamma D(G(x_s)) + (1 - \gamma)\alpha_F(i) \\ \alpha_R(i+1) = \gamma D(x_l) + (1 - \gamma)\alpha_R(i) \end{cases}, SE \leq i \leq TE \quad (9)$$

Here, γ is decay coefficient, and SE represents the starting epoch to implement LeCam regularization term, which is conducive to avoid the excessive regularization in the initial stage with under fitting.

D. Experimental evaluation

To validate the efficacy of the proposed augmentation method, we conducted intra-subject classification experiments with limited training data. Specifically, the original data from a target subject is divided into training set $\mathcal{T}_{tr}(X_s)$ and testing set $\mathcal{T}_{tt}(X_s)$. We exploit the two-stage training strategy to optimize the parameters of the generator G_t , and then employ it to transform the $\mathcal{T}_{tr}(X_s)$ and $\mathcal{T}_{tt}(X_s)$ into $\mathcal{T}_{tr}(X_l)$ and $\mathcal{T}_{tt}(X_l)$, respectively. Finally, the $\mathcal{T}_{tr}(X_l)$ is used to train four SSVEP classifiers as mentioned in Section 2.2, and undertake evaluation on $\mathcal{T}_{tt}(X_l)$. To eliminate the randomness of data partitioning, the K-Fold evaluation strategy was adopted in the experiments, under which the parameters of G_s remained unchanged while G_t was updated K times in the whole process.

In this study, we implemented the proposed augmentation method in PyTorch framework. The hyperparameters on two datasets are set as follows.

- Direction:** For the first training stage, mini-batch (B) = 64, epochs (E) = 200, learning rate (lr) = 0.001, optimizer (Opt) = Adam (beta1 = 0.9, beta2 = 0.999), weight decay (wd) = 0.0001. For the second training stage, B = 20, E = 500, lr = 0.01, Opt = Adam (beta1 = 0.9, beta2 = 0.999) + Cosine Annealing, wd

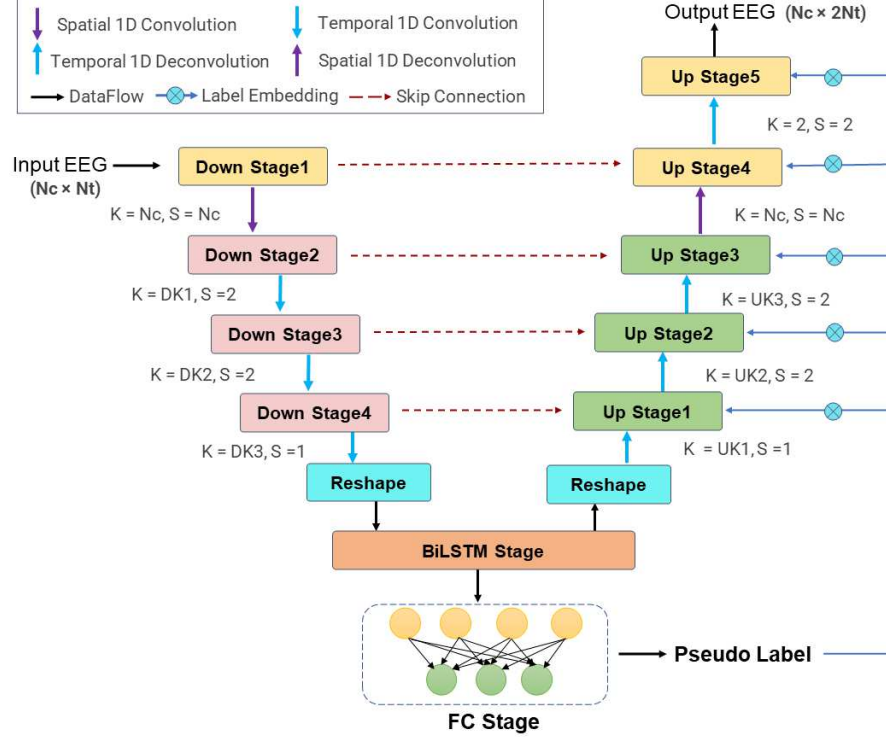


Fig. 2: The architecture of generator. The whole architecture of the generator follows the design of U-Net, which is divided into two stages: down sampling and up sampling. Where N_c is the number of EEG channels, N_t denotes the number of sample points. K, S represents the size of convolution/deconvolution kernel and stride, respectively. DK_i, UK_i ($i=1, 2, 3$) corresponding to kernel size for down sampling stage and up sampling stage, respectively.

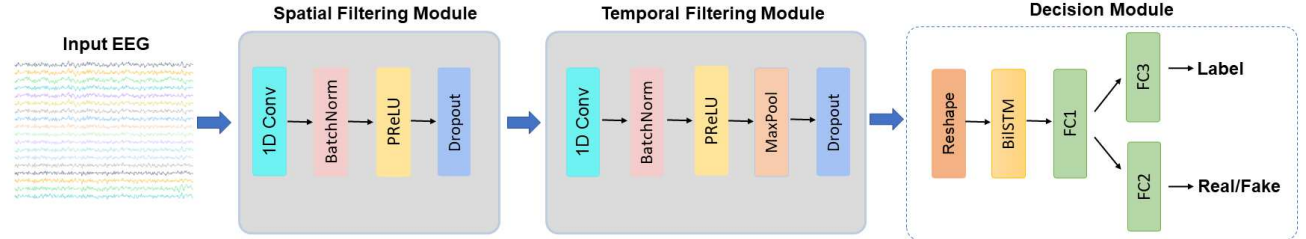


Fig. 3: The architecture of discriminator. The discriminator follows the design of SSVEPNet, which mainly comprised of a spatial filtering module, a temporal filtering module, and a decision module.

$= 0.0003$. For the regularization term, $SE = 50$, $\lambda = 0.6$, $\gamma = 0.90$.

- **Dial:** All hyperparameters are identical with Direction SSVEP dataset, except for the min-batch in the second training stage, which is set to 24 in this dataset.

E. Statistical analysis

In this study, classification accuracy was adopted as the evaluation metric. The average classification results across all subjects for K -times validation were presented in the form of mean \pm standard deviation. Two transformation scenarios, i.e. 0.5 s to 1 s and 1 s to 2 s, were analyzed in the experiments. Paired t-tests were implemented to investigate whether there were significant differences in the classification accuracy between all pairs of methods at each condition.

III. RESULTS

Firstly, we investigated the results of four baseline methods using limited training data. In this setting, the TEGAN that used to extend signal length was trained by 20% SSVEP data. **Fig. 4** shows the averaged classification results of original signals and augmented signals with different signal lengths across all subjects. We could observe that augmented signals yielded better classification performance than original signals on both two transformation scenarios, and the results of two SSVEP datasets manifest the consistent tendency. Interestingly, we could find that the augmented signals at 1.0 s have achieved better results than original signals at 1.0 s for three methods (ITCCA, EEGNet, and C-CNN).

Moreover, we investigated the results how the performance of four baseline methods varied with different scales of dataset. Specifically, the SSVEP dataset from each subject was divided into the training

TABLE I: The detailed network parameters of generator

Block	Module	Layer	Output	Description
Down Sampling	Input Module	Input	$(b, 1, N_c, N_t)$	$(batch_size, 1, num_channels, num_time_steps)$
		Conv1D	$(b, DC_i, 1, DT_i)$	$kernel = \{N_c, DK_1, DK_2, DK_3\}$ $stride = \{N_c, 2, 2, 1\}$ $C_i = 2^{i+1} * N_c, i = \{0, 1, 2, 3\}$ $DT_0 = N_t, DT_{i+1} = (DT_i - kernel[i]) // stride[i] + 1$ $max_norm (= 1.0) + BN, i = 0$ $SN [48] + BN, i = 1, 2, 3$
		Norm	$(b, DC_i, 1, DT_i)$	
		Activation	$(b, DC_i, 1, DT_i)$	PRelu [49]
	Reshape Module	Dropout	$(b, DC_i, 1, DT_i)$	$p = 0.5$
	Reshape	(b, DT_3, DC_3)		
BiLSTM Encoding	BiLSTM Module	LSTM	$(b, 2 * DT_3, DC_3)$	$input_size, hidden_size = DC_3, num_layers = 1$ $batch_first = True, bidirectional = True$
		Reshape	$(b, 1, 2 * DT_3 * DC_3)$	
		AvgPool	$(b, 1, DT_3 * DC_3)$	$kernel = 2, stride = 2$
Pseudo Label Generation	FC Module	Flatten	$(b, DT_3 * DC_3)$	
		Linear	(b, K)	SN
		Norm	(b, K)	
Up Sampling	Selection Module	Argmax	$(b, 1)$	select the highest probability as pseudo label
		Reshape Module	$(b, DC_3, 1, DT_3)$	
Up Sampling	UpStage Module($\times 5$)	DeConv1D	$(b, UC_i, 1, UT_i)$	$kernel = \{UK_1, UK_2, UK_3, N_c, 2\}$ $stride = \{1, 2, 2, N_c, 2\}$ $UC = \{8 * N_c, 8 * N_c, 4 * N_c, 2 * N_c, N_c\}$ $UT = \{DT_2, DT_1, DT_0, N_t, 2 * N_t\}$ $SN + cBN [50]$ $PRelu$
		Norm	$(b, UC_i, 1, UT_i)$	
		Activation	$(b, UC_i, 1, UT_i)$	
		Conv1D	$(b, UC_i // M_i, 1, UT_i)$	$kernel = 1, stride = 1, M = \{0, 2, 2, 2, N_c\}$ only exist when $i \geq 1$
		Norm	$(b, UC_i // M_i, 1, UT_i)$	$SN + cBN, only exist when i \geq 1$
		Activation	$(b, UC_i // M_i, 1, UT_i)$	$PRelu, only exist when i \geq 1$
	Output Module	Output	$(b, 1, N_c, 2 * N_t)$	

dataset and testing dataset in the portion of 2:8, 5:5 and 8:2 respectively. In this study, we marked these three scales of datasets as small-scale, middle-scale and large-scale dataset. Fig. 5 illustrates averaged classification results across subjects of four baseline classification methods using original signals and augmented signals at different scales of datasets on two SSVEP datasets. With the continuous expansion of training data, the average classification performance of each baseline algorithm for the original signal and the augmented signal has been gradually improved, and the trend is consistent on both two SSVEP datasets. In addition, the augmented signal improves the classification performance on a small-scale training dataset more significantly. With the continuous expansion of training data, the improvement effect of classification performance of augmented signals is gradually weakened. More interestingly, when original signals were converted to augmented signal by TEGAN on any scale of dataset, the classification performance gap of all algorithms is significantly reduced.

Furthermore, we conducted ablation experiments on the Dial SSVEP dataset to explore the contribution of pivotal component to implement the augmentation framework. The augmented data at 2.0 s was generated by original data at 1.0 s, and the signal converter TEGAN was trained by 20% training data. Four modules, i.e. auxiliary classifier in the discriminator, the pseudo-label generation in the generator, the two-stage training strategy, and the LeCam divergence regularization term were investigated in this study. As shown in Table II, the averaged classification results indicate that four important components of TEGAN are all helpful to improve the classification performance of augmented data. It is worth noting that after removing the two-stage training strategy from TEGAN, the model would be trained using only 20% data of target subject.

IV. DISCUSSION

In recent years, enhancing the classification performance of SSVEPs with limited calibration data is a hot research topic, which empower the practicality of various BCI applications [32], [53]–[55]. To this end, modelling an efficient classification method requiring less calibration data or create supplemented synthetic data to enlarge the size of the training dataset are most commonly strategies. Nevertheless, in this study, we proposed a novel pipeline that leverage the subject-invariant properties of SSVEPs to address this issue. Specifically, we developed a GAN-based model, i.e., TEGAN, which could be used to extend the data length of SSVEP data. TEGAN seeks to learn the mapping relationship between short-time and long-time signals through an adversarial game training paradigm. Concretely, the generator is responsible for extracting signal features from the short-time SSVEP data and reconstructing the long-time SSVEP data. The discriminator assists the generator to improve the quality of the generated data by learning the discrepancy information between the real and fake long-time signal.

After analyzing the result in Table II, we could conclude that the two-stage training strategy plays an indispensable role in enhancing the performance of TEGAN. However, although the two-stage training strategy can greatly improve BCI performance with only a small amount of target subject data, it still suffers the laborious calibration procedure. Implementing a high-performance BCI system with zero calibration for new users has always been the ultimate goal of the BCI community. In this study, we verify the feasibility via improving the performance of training-free methods. Concretely, we employ the cross-subject data to train TEGAN, and then use it to extend the signal length of target data. Two representative methods as

TABLE II: Ablation study on Dial SSVEP Dataset.

Case	Module Selection					Accuracy(%)			
	Auxiliary Classifier	Pseudo Label	Two Stage	LeCam Divergence		ITCCA	TRCA	EEGNet	C-CNN
(a)	—	✓	✓	✓		80.56±18.86**	72.26±15.23***	79.70±17.90**	79.68±18.63**
(b)	✓	—	✓	✓		84.24±18.40	78.61±19.82	71.57±23.59***	83.93±18.53
(c)	✓	✓	—	✓		74.40±23.34**	76.92±22.24	78.14±22.47*	78.24±22.47*
(d)	✓	✓	✓	—		79.22±19.92**	74.43±19.44***	78.72±20.02**	79.41±18.91**
(e)	✓	✓	✓	✓		84.61±16.54	82.44±17.19	83.54±17.40	84.15±16.91

‘—’ denotes which module is deleted from the proposed GAN model, and ‘✓’ denotes which module is remained. The asterisk in the table indicate significant difference between each pair of the two methods by paired t-tests (* $p < 0.05$, ** $p < 0.01$, *** $p < 0.001$)

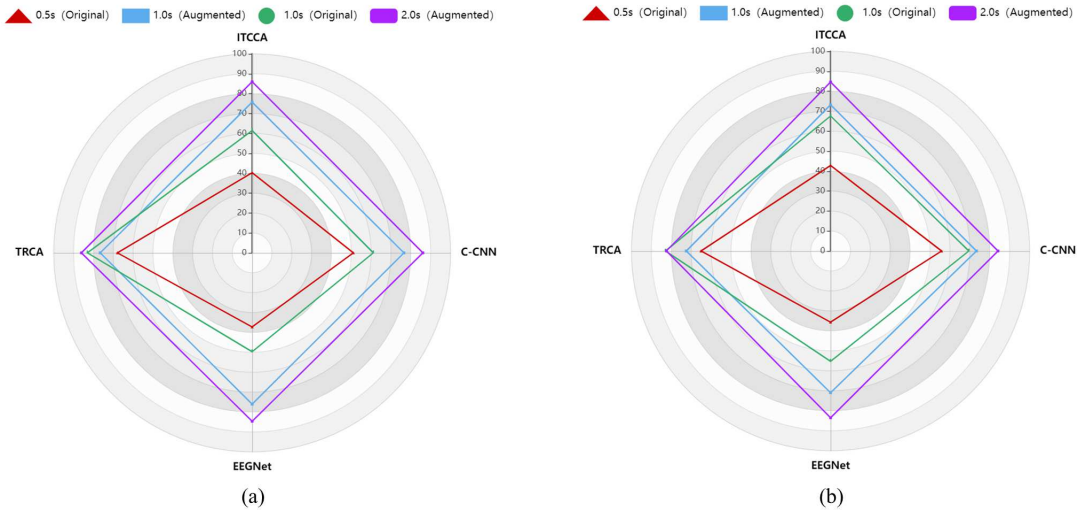


Fig. 4: Averaged classification results of original signals and augmented signals with different signal lengths across all subjects. Four baseline classification methods as ITCCA, TRCA, EEGNet and C-CNN were validated on (a) Direction SSVEP Dataset, (b) Dial SSVEP Dataset. On each dataset, the original signal length was set to 0.5 s and 1.0 s, corresponding to their augmented signal length 1.0 s and 2.0 s.

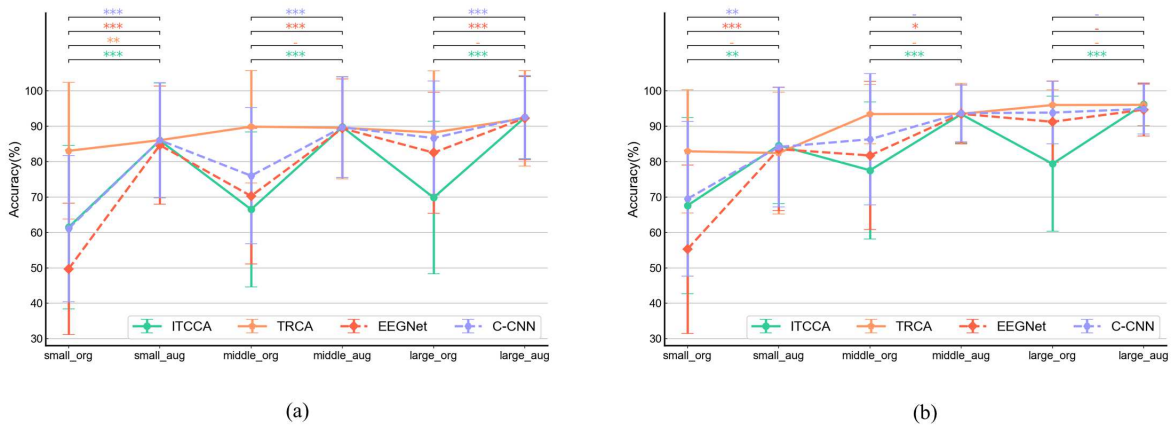


Fig. 5: Averaged classification results across subjects of four baseline classification methods as ITCCA, TRCA, EEGNet and C-CNN using original signals and augmented signals at different scales of datasets on (a) Direction SSVEP Dataset, (b) Dial SSVEP Dataset. On each dataset, the original signal length was set to 1.0 s, corresponding to its augmented signal length 2.0 s. The colored asterisk in the figure indicates significant difference between original signals and augmented signals at this scale of dataset by paired t-tests (* $p < 0.05$, ** $p < 0.01$, *** $p < 0.001$).

CCA and MSI were selected to conduct evaluation. [Fig. 6](#) illustrates the averaged classification result across all subjects of two methods on two SSVEP datasets. The results demonstrate the TEGAN could significantly improve the performance of CCA and MSI on both SSVEP datasets. Especially in the transformation scenario of 0.5 s to 1.0 s on Direction SSVEP dataset, the classification performance of CCA and MSI has nearly doubled. The impressive result substantiates the great potential of using TEGAN to assist unsupervised algorithms for implementing high-performance zero-calibration BCI systems.

From [Fig. 4](#) and [Fig. 5](#), we can find an interesting phenomenon that reconstructed long-time SSVEP signals are capable of reducing the performance gap among various classification methods. To explain this phenomenon, we visualize extracted features of a representative subject (subject 5 on Dial SSVEP Dataset) for four baseline classification methods. It can be observed from [Fig. 7](#) that there is a large gap in the features extracted from each category on the original signals, while the gap is gradually narrowed on the augmented signals. Specifically, for the classification algorithms that previously had not obvious features of the target stimulus on the original signal, the features were further amplified on the augmented signals. In other words, the augmented signals possess more discriminative or representative features of the target stimulus compared to the original signal, which makes it easier for the classification algorithm to distinguish between target and non-target stimuli and thus facilitates the improvement of the classification performance.

Extensive studies have proved the significance of filter bank technologies in enhancing the recognition performance of SSVEPs [10], [22], [33], [56]–[58]. The filter bank technology is based on the premise that the brain-generated SSVEP signal has a distinctive peak at the harmonic or subharmonic frequency of the flash stimulus. Generally, the amplitude of the fundamental frequency peak in the SSVEP signal is higher than that of the harmonic and subharmonic peaks [59]. For the information fusion process of different frequency bands of filter bank technology, the frequency band where the fundamental wave is located has a higher weight, while the frequency band where the harmonic wave is located has a lower weight. However, based on the particularity that the harmonic component or subharmonic component of SSVEP signal is not obvious, we speculate that this feature would bring great trouble to GAN in the process of learning to generate SSVEP data. Deep neural networks may tend to preferentially capture the fundamental frequency information with dominated characteristics, while ignoring the harmonic and subharmonic information with less obvious characteristics. To verify this hypothesis, we made a comparison of time and frequency domain representation between real SSVEP data and generated SSVEP data. The TEGAN was trained by 20% SSVEP data, and two frequencies (6.67 Hz and 12.0 Hz) were chosen for evaluation. As shown in [Fig. 8](#), we could observe that the amplitude and trend of the original SSVEP signal and the generated SSVEP signal at the two frequencies differ sufficiently in the time domain. In addition, both the original signal and the generated signal have significant peaks on the fundamental frequency in the frequency domain characterization, while the identifiable harmonic components contained in the original signal are hard to reproduce in the generated signal.

According to the limitations and challenges of current study, at least the following aspects could be further improved in the future. Firstly, to the best of our knowledge, this is the first research using GAN technology to generate more than 10 categories of SSVEP data (Dial SSVEP dataset). However, with the increasing number of categories, it would become extremely difficult for GAN to simulate the real data distribution. Therefore, we should strive to generate SSVEP data with more categories, such as Benchmark [60] and BETA dataset [61]. Secondly, in this paper, our GAN model could only expand the

length of the original signal twice. In the subsequent research, we could further improve the network architecture of TEGAN, enabling it to expand more multiples of the signal length. Moreover, filter bank technology should be incorporated in the framework design as well, which could help the GAN model excavate the harmonic information that has an important contribution to the identification process, thus improving the quality of generated data. Last but not least, the most advanced transfer learning technique, such as improved two-stage training strategy [62], could be utilized to build a high-performance BCI system with shorter calibration time.

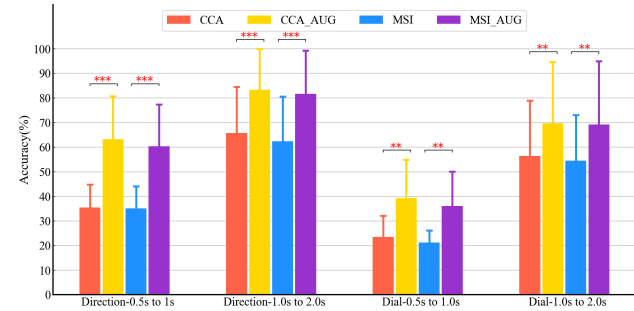


[Fig. 6](#): Averaged classification results across subjects of two training-free classification methods as CCA, MSI using original signals and augmented signals on Direction and Dial SSVEP dataset. The red asterisk in the figure indicates significant difference between original signals and augmented signals at this transformation scenario by paired t-tests (** $p < 0.01$, *** $p < 0.001$)

V. CONCLUSION

Building a high-performance SSVEP-BCI system with limited calibration data is an urgent demand for the BCI community. In this study, we proposed a novel GAN-based augmentation strategy to enhance the performance of SSVEP-based BCI. Rather than simply enlarging the training dataset, the proposed augmentation method served as a signal converter that could be employed to extend data length. Experimental results based on a 4-class and a 12-class SSVEP datasets demonstrate that the proposed augmentation method could significantly improve the recognition accuracy of traditional methods and deep learning methods with limited subject-specific data. Furthermore, it holds transformative promise to build a high-performance SSVEP-BCI system with zero-calibration procedure for new users. Overall, the proposed augmentation method could significantly shorten the calibration time and uncover the underlying subject-invariant properties of SSVEP data, which facilitates the implementation of various SSVEP-based BCI applications.

ACKNOWLEDGEMENT

This work was supported in part by the National Natural Science Foundation of China under Grant No.62076209.

REFERENCES

- [1] J. R. Wolpaw *et al.*, “Brain-computer interface technology: a review of the first international meeting,” *IEEE transactions on rehabilitation engineering*, vol. 8, no. 2, pp. 164–173, 2000.
- [2] H.-J. Hwang, S. Kim, S. Choi, and C.-H. Im, “Eeg-based brain-computer interfaces: a thorough literature survey,” *International Journal of Human-Computer Interaction*, vol. 29, no. 12, pp. 814–826, 2013.
- [3] R. Abiri, S. Borhani, E. W. Sellers, Y. Jiang, and X. Zhao, “A comprehensive review of eeg-based brain–computer interface paradigms,” *Journal of neural engineering*, vol. 16, no. 1, p. 011001, 2019.

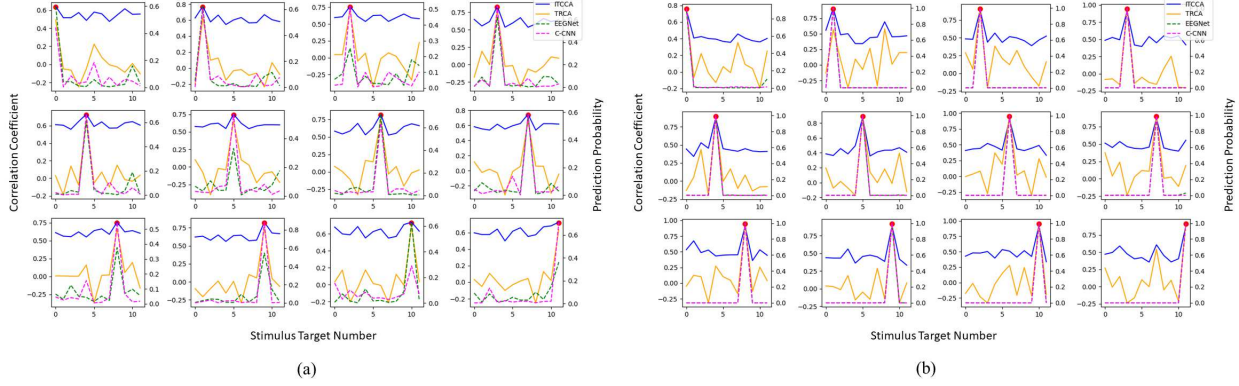


Fig. 7: The features of a representative subject (subject 5 on Dial SSVEP Dataset) for four baseline classification methods as ITCCA, TRCA, EEGNet and C-CNN. ITCCA, TRCA use the correlation coefficients as features, while the prediction probabilities are treated as features by EEGNet and C-CNN. (a) Original signals at 1.0 s, (b) Augmented signals at 2.0 s. Red dot marks the correlation coefficient or prediction probability at the frequency of gaze following target.

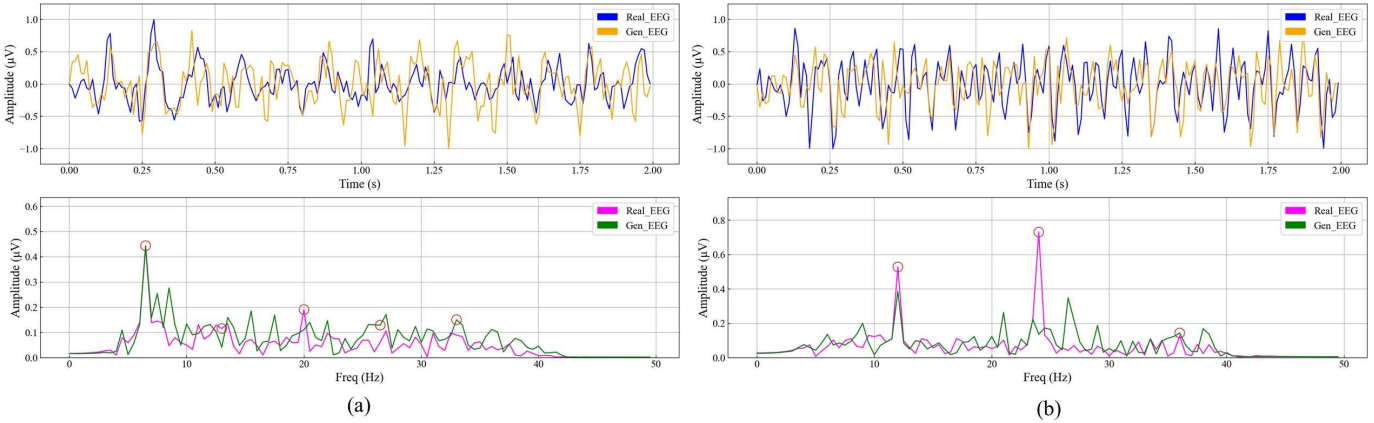


Fig. 8: Comparison of time and frequency domain representation at Oz channel of a representative subject (subject 30 on Direction SSVEP Dataset) between real EEG data and generated EEG data. (a) SSVEP signal at 6.67 Hz, (b) SSVEP signal at 12 Hz. The time window for the real EEG data is 2.0 s, while the generated data is transformed from the real EEG data at 1.0 s. In the frequency domain representation, red circles mark the fundamental frequency or harmonics.

- [4] K. K. Ang *et al.*, “Filter bank common spatial pattern (fbcsp) in brain–computer interface,” in *2008 IEEE international joint conference on neural networks (IEEE world congress on computational intelligence)*, pp. 2390–2397, IEEE, 2008.
- [5] F. Nijboer *et al.*, “A p300-based brain–computer interface for people with amyotrophic lateral sclerosis,” *Clinical neurophysiology*, vol. 119, no. 8, pp. 1909–1916, 2008.
- [6] D.-W. Kim *et al.*, “Classification of selective attention to auditory stimuli: toward vision-free brain–computer interfacing,” *Journal of neuroscience methods*, vol. 197, no. 1, pp. 180–185, 2011.
- [7] Z. Lin *et al.*, “Frequency recognition based on canonical correlation analysis for ssvep-based bcis,” *IEEE transactions on biomedical engineering*, vol. 53, no. 12, pp. 2610–2614, 2006.
- [8] J.-H. Lim, H.-J. Hwang, C.-H. Han, K.-Y. Jung, and C.-H. Im, “Classification of binary intentions for individuals with impaired oculomotor function:‘eyes-closed’ssvep-based brain–computer interface (bci),” *Journal of neural engineering*, vol. 10, no. 2, p. 026021, 2013.
- [9] N.-S. Kwak *et al.*, “A convolutional neural network for steady state visual evoked potential classification under ambulatory environment,” *PLoS one*, vol. 12, no. 2, p. e0172578, 2017.
- [10] W. Dang *et al.*, “Mhlccn: Multi-harmonic linkage cnn model for ssvep and ssmvep signal classification,” *IEEE Transactions on Circuits and Systems II: Express Briefs*, vol. 69, no. 1, pp. 244–248, 2021.
- [11] M. Nakanishi *et al.*, “A comparison study of canonical correlation analysis based methods for detecting steady-state visual evoked potentials,” *PLoS one*, vol. 10, no. 10, p. e0140703, 2015.
- [12] X. Chen *et al.*, “High-speed spelling with a noninvasive brain–computer interface,” *Proceedings of the national academy of sciences*, vol. 112, no. 44, pp. E6058–E6067, 2015.
- [13] M. Kim *et al.*, “Online home appliance control using eeg-based brain–computer interfaces,” *Electronics*, vol. 8, no. 10, p. 1101, 2019.
- [14] E. C. Lalor *et al.*, “Steady-state vep-based brain–computer interface control in an immersive 3d gaming environment,” *EURASIP Journal on Advances in Signal Processing*, vol. 2005, no. 19, pp. 1–9, 2005.
- [15] R. Zerafa *et al.*, “To train or not to train? a survey on training of feature extraction methods for ssvep-based bcis,” *Journal of Neural Engineering*, vol. 15, no. 5, p. 051001, 2018.
- [16] Y. Zhang *et al.*, “Multivariate synchronization index for frequency recognition of ssvep-based brain–computer interface,” *Journal of neuroscience methods*, vol. 221, pp. 32–40, 2014.
- [17] Y. Chen *et al.*, “Implementing a calibration-free ssvep-based bci system with 160 targets,” *Journal of Neural Engineering*, vol. 18, no. 4, p. 046094, 2021.
- [18] G. Bin *et al.*, “A high-speed bci based on code modulation vep,” *Journal of neural engineering*, vol. 8, no. 2, p. 025015, 2011.
- [19] Y. Zhang *et al.*, “Multiway canonical correlation analysis for frequency components recognition in ssvep-based bcis,” in *International Conference on Neural information processing*, pp. 287–295, Springer, 2011.
- [20] M. Nakanishi *et al.*, “Enhancing detection of ssveps for a high-speed brain speller using task-related component analysis,” *IEEE Transactions on Biomedical Engineering*, vol. 65, no. 1, pp. 104–112, 2017.
- [21] Y. Zhang *et al.*, “Correlated component analysis for enhancing the performance of ssvep-based brain–computer interface,” *IEEE Transac-*

tions on Neural Systems and Rehabilitation Engineering, vol. 26, no. 5, pp. 948–956, 2018.

[22] X. Chen *et al.*, “Filter bank canonical correlation analysis for implementing a high-speed ssvep-based brain–computer interface,” *Journal of neural engineering*, vol. 12, no. 4, p. 046008, 2015.

[23] P. Yuan *et al.*, “Enhancing performances of ssvep-based brain–computer interfaces via exploiting inter-subject information,” *Journal of neural engineering*, vol. 12, no. 4, p. 046006, 2015.

[24] N. R. Waytowich *et al.*, “Unsupervised adaptive transfer learning for steady-state visual evoked potential brain–computer interfaces,” in *2016 IEEE International Conference on Systems, Man, and Cybernetics (SMC)*, pp. 004135–004140, IEEE, 2016.

[25] K.-J. Chiang *et al.*, “Boosting template-based ssvep decoding by cross-domain transfer learning,” *Journal of Neural Engineering*, vol. 18, no. 1, p. 016002, 2021.

[26] C. M. Wong *et al.*, “Inter-and intra-subject transfer reduces calibration effort for high-speed ssvep-based bcis,” *IEEE Transactions on Neural Systems and Rehabilitation Engineering*, vol. 28, no. 10, pp. 2123–2135, 2020.

[27] C. M. Wong *et al.*, “Transferring subject-specific knowledge across stimulus frequencies in ssvep-based bcis,” *IEEE Transactions on Automation Science and Engineering*, vol. 18, no. 2, pp. 552–563, 2021.

[28] W. Yan *et al.*, “Cross-subject spatial filter transfer method for ssvep–eeg feature recognition,” *Journal of Neural Engineering*, vol. 19, no. 3, p. 036008, 2022.

[29] N. Waytowich *et al.*, “Compact convolutional neural networks for classification of asynchronous steady-state visual evoked potentials,” *Journal of neural engineering*, vol. 15, no. 6, p. 066031, 2018.

[30] A. Ravi *et al.*, “Comparing user-dependent and user-independent training of cnn for ssvep bci,” *Journal of neural engineering*, vol. 17, no. 2, p. 026028, 2020.

[31] O. B. Guney *et al.*, “A deep neural network for ssvep-based brain–computer interfaces,” *IEEE Transactions on Biomedical Engineering*, vol. 69, no. 2, pp. 932–944, 2021.

[32] Y. Pan *et al.*, “An efficient cnn-lstm network with spectral normalization and label smoothing technologies for ssvep frequency recognition,” *Journal of Neural Engineering*, vol. 19, no. 5, p. 056014, 2022.

[33] J. Chen *et al.*, “A transformer-based deep neural network model for ssvep classification,” *arXiv preprint arXiv:2210.04172*, 2022.

[34] R. Luo *et al.*, “Data augmentation of ssveps using source aliasing matrix estimation for brain–computer interfaces,” *IEEE Transactions on Biomedical Engineering*, 2022.

[35] S. Thirumuruganathan *et al.*, “Approximate query processing for data exploration using deep generative models,” in *2020 IEEE 36th international conference on data engineering (ICDE)*, pp. 1309–1320, IEEE, 2020.

[36] T. Salimans *et al.*, “Pixelcnn++: Improving the pixelcnn with discretized logistic mixture likelihood and other modifications,” *arXiv preprint arXiv:1701.05517*, 2017.

[37] D. P. Kingma *et al.*, “Auto-encoding variational bayes,” *arXiv preprint arXiv:1312.6114*, 2013.

[38] I. Goodfellow *et al.*, “Generative adversarial nets,” *Advances in neural information processing systems*, vol. 27, 2014.

[39] J. Ho *et al.*, “Denoising diffusion probabilistic models,” *Advances in Neural Information Processing Systems*, vol. 33, pp. 6840–6851, 2020.

[40] K. G. Hartmann *et al.*, “Eeg-gan: Generative adversarial networks for electroencephalographic (eeg) brain signals,” *arXiv preprint arXiv:1806.01875*, 2018.

[41] N. K. N. Aznan *et al.*, “Simulating brain signals: Creating synthetic eeg data via neural-based generative models for improved ssvep classification,” in *2019 International Joint Conference on Neural Networks (IJCNN)*, pp. 1–8, IEEE, 2019.

[42] N. K. N. Aznan *et al.*, “Leveraging synthetic subject invariant eeg signals for zero calibration bci,” in *2020 25th International Conference on Pattern Recognition (ICPR)*, pp. 10418–10425, IEEE, 2021.

[43] J. Kwon *et al.*, “Novel signal-to-signal translation method based on star-gan to generate artificial eeg for ssvep-based brain–computer interfaces,” *Expert Systems with Applications*, p. 117574, 2022.

[44] M.-H. Lee *et al.*, “Eeg dataset and openbmi toolbox for three bci paradigms: An investigation into bci illiteracy,” *GigaScience*, vol. 8, no. 5, p. giz002, 2019.

[45] H. Tanaka, T. Katura, and H. Sato, “Task-related component analysis for functional neuroimaging and application to near-infrared spectroscopy data,” *NeuroImage*, vol. 64, pp. 308–327, 2013.

[46] V. J. Lawhern *et al.*, “Eegnet: a compact convolutional neural network for eeg-based brain–computer interfaces,” *Journal of neural engineering*, vol. 15, no. 5, p. 056013, 2018.

[47] A. Odena *et al.*, “Conditional image synthesis with auxiliary classifiers,” in *International conference on machine learning*, pp. 2642–2651, PMLR, 2017.

[48] T. Miyato *et al.*, “Spectral normalization for generative adversarial networks,” *arXiv preprint arXiv:1802.05957*, 2018.

[49] K. He *et al.*, “Delving deep into rectifiers: Surpassing human-level performance on imagenet classification,” December 2015.

[50] V. Dumoulin *et al.*, “A learned representation for artistic style,” *arXiv preprint arXiv:1610.07629*, 2016.

[51] O. Ronneberger *et al.*, “U-net: Convolutional networks for biomedical image segmentation,” in *International Conference on Medical image computing and computer-assisted intervention*, pp. 234–241, Springer, 2015.

[52] H.-Y. Tseng *et al.*, “Regularizing generative adversarial networks under limited data,” in *Proceedings of the IEEE/CVF Conference on Computer Vision and Pattern Recognition*, pp. 7921–7931, 2021.

[53] C. M. Wong *et al.*, “Learning across multi-stimulus enhances target recognition methods in ssvep-based bcis,” *Journal of neural engineering*, vol. 17, no. 1, p. 016026, 2020.

[54] Z. Wang *et al.*, “Stimulus-stimulus transfer based on time-frequency-joint representation in ssvep-based bcis,” *IEEE Transactions on Biomedical Engineering*, 2022.

[55] T. Jorajuria *et al.*, “Oscillatory source tensor discriminant analysis (ostda): A regularized tensor pipeline for ssvep-based bci systems,” *Neurocomputing*, vol. 492, pp. 664–675, 2022.

[56] W. Ding *et al.*, “Filter bank convolutional neural network for short time-window steady-state visual evoked potential classification,” *IEEE Transactions on Neural Systems and Rehabilitation Engineering*, vol. 29, pp. 2615–2624, 2021.

[57] H. Yao *et al.*, “Fb-eegnet: A fusion neural network across multi-stimulus for ssvep target detection,” *Journal of Neuroscience Methods*, vol. 379, p. 109674, 2022.

[58] P. R. Bassi *et al.*, “Fbdnn: filter banks and deep neural networks for portable and fast brain–computer interfaces,” *Biomedical Physics & Engineering Express*, vol. 8, no. 3, p. 035018, 2022.

[59] R. Zhang, Z. Xu, L. Zhang, L. Cao, Y. Hu, B. Lu, L. Shi, D. Yao, and X. Zhao, “The effect of stimulus number on the recognition accuracy and information transfer rate of ssvep–bci in augmented reality,” *Journal of Neural Engineering*, vol. 19, no. 3, p. 036010, 2022.

[60] Y. Wang *et al.*, “A benchmark dataset for ssvep-based brain–computer interfaces,” *IEEE Transactions on Neural Systems and Rehabilitation Engineering*, vol. 25, no. 10, pp. 1746–1752, 2016.

[61] B. Liu *et al.*, “Beta: A large benchmark database toward ssvep-bci application,” *Frontiers in neuroscience*, vol. 14, p. 627, 2020.

[62] O. B. Guney *et al.*, “Transfer learning of an ensemble of dnns for ssvep bci spellers without user-specific training,” *Journal of Neural Engineering*, 2022.